Turk Neurosurg 36(3):457-466, 2026
DOI: 10.5137/1019-5149.JTN.49456-25.2

Original Investigation

Neuroanatomy

Received: 16.07.2025
Accepted: 29.09.2025

Published Online: 22.05.2026

Endoscopic Endonasal Approach to Identify the Medial Corridor of the Cavernous Sinus: A Cadaveric Study with Clinical Correlation

Aykut GOKBEL[1], Ayse UZUNER[2], Eren YILMAZ[1], Atakan EMENGEN[3], Musa CIRAK[4], Burak CABUK[5], Ihsan ANIK[5], Savas CEYLAN[3]

[1]Istinye University, Department of Neurosurgery, Istanbul, Türkiye
[2]Afşin State Hospital, Department of Neurosurgery, Kahramanmaras, Türkiye
[3]Bahcesehir University School of Medicine, Department of Neurosurgery, Istanbul, Türkiye
[4]Bakirkoy Dr. Sadi Konuk Training and Research Hospital, Department of Neurosurgery, Istanbul, Türkiye
[5]Kocaeli University School of Medicine, Department of Neurosurgery, Kocaeli, Türkiye

Corresponding author: Savas CEYLAN ✉ ssceylan@yahoo.com

ABSTRACT

AIM: To define the existence and precise anatomical boundaries of the medial corridor (MC) within the cavernous sinus (CS), using an endoscopic endonasal transsphenoidal approach, and to correlate these anatomical findings with clinical patterns of CS invasion in patients with pituitary adenomas.

MATERIAL and METHODS: An endoscopic endonasal transsphenoidal technique was used to perform anatomical dissections on 10 CSs obtained from 5 adult cadaveric heads. Key neurovascular landmarks were systematically identified, and quantitative measurements of their spatial relationships were recorded. To establish clinical relevance, anatomical observations were correlated with radiological and intraoperative findings from 20 patients with pituitary adenomas demonstrating CS invasion on preoperative imaging.

RESULTS: The MC was consistently identified in all cadaveric specimens, confirming its reproducible anatomical presence. The mean distance between the anterior genu of the internal carotid artery (ICA) and the pituitary gland was 5.0 ± 1.5 mm. Clinical correlations revealed that pituitary adenomas preferentially invade the superior compartment of the CS via the MC prior to lateral and posterior extension. The oculomotor nerve (cranial nerve III) was a reliable anatomical landmark defining the lateral boundary of the MC.

CONCLUSION: Comprehensive anatomical delineation of the MC is critical for refining endoscopic surgical strategies, maximizing the extent of safe tumor resection, and minimizing neurovascular morbidity. The consistently identified interval of approximately 5 mm between the anterior genu of the ICA and the pituitary gland provides a robust and practical intraoperative reference point for safe navigation through the MC of the CS.

KEYWORDS: Cavernous sinus, Pituitary adenoma, Internal carotid artery, Endoscopic surgical procedure

ABBREVIATIONS: 3D: Three-dimensional, **C4:** Cavernous segment, **CN:** Cranial nerve, **CS:** Cavernous sinus, **EETA:** Endoscopic endonasal transsphenoidal approach, **ICA:** Internal carotid artery, **MC:** Medial corridor, **SOF:** Superior orbital fissure

Aykut GOKBEL : 0000-0002-9332-3321
Ayse UZUNER : 0000-0002-6471-7452
Eren YILMAZ : 0000-0002-5911-7268
Atakan EMENGEN : 0000-0002-6853-1540
Musa CIRAK : 0000-0002-0175-9655
Burak CABUK : 0000-0003-1198-3869
Ihsan ANIK : 0000-0003-2567-7969
Savas CEYLAN : 0000-0002-2747-8907

INTRODUCTION

Over the past two decades, the progressive evolution of transsphenoidal surgical techniques has greatly advanced the understanding of skull base anatomy. In particular, the integration of endoscopic visualization into transsphenoidal surgery has enabled unparalleled exposure of the deep and previously concealed anatomical regions surrounding the sella turcica, including the planum sphenoidale, clivus, and neurovascular prominences of the optic nerves and internal carotid arteries (4,15). These advancements have not only expanded the anatomical reach of endonasal approaches but also fundamentally reshaped surgical paradigms for lesions involving the parasellar and cavernous regions.

Among these regions, the cavernous sinus (CS) is one of the most anatomically complex and surgically challenging structures of the skull base. Its dense neurovascular content, intricate venous architecture, and intimate relationship with the internal carotid artery (ICA) necessitate a precise and compartmentalized anatomical understanding to ensure surgical safety and efficacy (8). Classical anatomical descriptions by Harris and Rhoton subdivided the CS into four venous regions, namely, anteroinferior (ventral), posterosuperior (dorsal), medial, and lateral, based on their spatial relationships with the ICA (14). Subsequent refinements by Fernandez-Miranda et al. proposed a compartmental framework consisting of superior, posterior, lateral, and inferior regions, which again considered the cavernous ICA (12). More recently, Ceylan et al. further refined this anatomical concept by identifying four distinct compartments, namely, superior, lateral, anteroinferior, and posterior, underscoring the evolving and dynamic nature of CS anatomy (3).

From a surgical perspective, endoscopic approaches to the CS have converged on the definition of two principal operative corridors, namely, the medial corridor (MC) and lateral corridor (7). The MC of the ICA is formed by the C-shaped cavernous segment (C4) of the artery and is medially constrained by the dorsum sellae, providing a potential pathway for medial-to-lateral access. Conversely, the lateral corridor is bounded posteriorly by the cavernous ICA, inferiorly by the vidian nerve, and anteriorly by the medial pterygoid prominence (5). Consistent with this corridor-based concept, Fernandez-Miranda et al. characterized the CS as comprising two principal wall structures, namely, the medial and lateral walls, with each assuming distinct surgical relevance depending on the chosen approach (11). Notably, the medial wall represents the primary interface encountered during endoscopic endonasal surgery, whereas the lateral wall is more frequently addressed via transcranial routes.

Accumulating anatomical and clinical evidence suggests that pituitary adenomas preferentially invade the CS through involvement of the medial wall. Our previous work has demonstrated that medial wall infiltration or compression constitutes a defining feature of CS invasion. However, medial wall disruption alone does not fully explain the observed patterns of tumor extension. Rather, engagement of the venous trabecular network located posterior to the medial wall appears to serve as a critical permissive factor that facilitates tumor progression into the CS (3,5,6). This observation highlights a complex, multistep mechanism of invasion that extends beyond simple wall penetration.

Against this backdrop, the present study was designed to precisely delineate the presence and anatomical boundaries of the MC using the endoscopic endonasal transsphenoidal approach (EETA) while simultaneously elucidating its role in the pathophysiology of CS invasion by pituitary adenomas. A refined understanding of the MC is essential for strategic surgical planning, reduction of neurovascular morbidity, and maximization of safe tumor resection. By integrating meticulous anatomical dissection with clinical correlation, this study aims to further clarify the anatomical–surgical interface of the CS and to contribute to the ongoing refinement of endoscopic skull base surgery.

MATERIAL and METHODS

This anatomical study examined 10 CSs obtained from five adult cadaveric heads. Specimens were either freshly frozen or prepared using arterial silicone injection to enhance vascular visualization. All dissections were performed at the Bahcesehir University Rhoton Laboratory. The study was conducted in accordance with the principles of the Declaration of Helsinki and was approved by the Local Ethics Committee of the Kocaeli University Faculty of Medicine (approval number: KAEK-233; September 20, 2017).

Both three-dimensional (3D) and two-dimensional digital video data were obtained during the dissections. Two-dimensional imaging was performed using 0° and 30° rigid endoscopes (Karl Storz, Tuttlingen, Germany), whereas stereoscopic visualization was achieved using the XION 3D endoscopic imaging system (XION, Berlin, Germany). The 3D endoscopy setup consisted of a MATRIX P Spectar camera processor (XION), a high-definition 3D camera head, and 3D endoscopes with diameters of 2.7 mm and 4 mm.

All endoscopic dissections were conducted through the right nasal cavity using a standard EETA. Following entry into the right nostril, key intranasal landmarks, including the nasal septum and the inferior, middle, and superior nasal turbinates, were systematically identified. The choana and sphenoethmoidal recess were visualized along the medial turbinate and nasal septum. After bilateral identification of the sphenoid ostia, the sphenoid sinus was entered via drilling, and an anterior sphenoidotomy was performed using a binostril technique.

Subsequently, critical skull base landmarks were exposed, including the sellar floor, planum sphenoidale anteriorly, clivus inferiorly, and prominences of the optic nerve and ICA laterally, along with the opticocarotid recesses. The lateral anatomical limits accessible through the endoscopic approach were carefully delineated. The superior sellar wall was opened using a high-speed drill, followed by bone removal and enlargement with a Kerrison rongeur. After dural opening, the anatomical boundaries of the MC were directly visualized.

A complete EETA was employed to define the surgical limits using natural nasal corridors, without the need for any external incisions on the cadaveric specimens. The bone overlying the

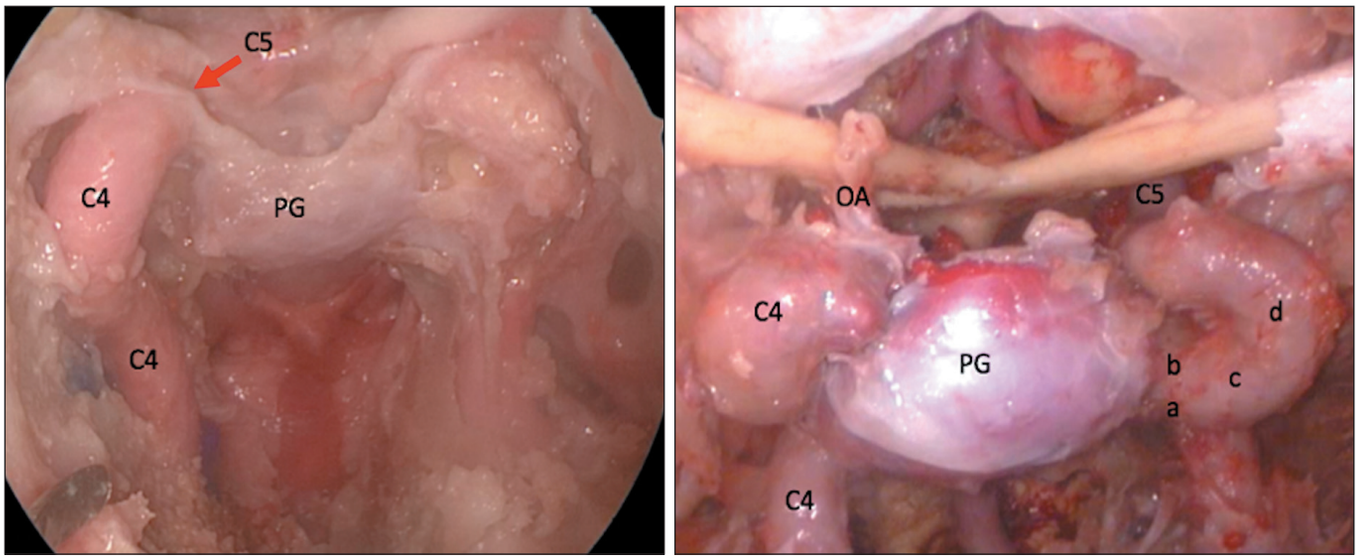

Figure 1: Cavernous (C4) and clinoid (C5) segments of the internal carotid artery; a: short vertical segment, b: posterior genu, c: horizontal segment, d: anterior genu. **PG:** pituitary gland, **OA:** ophthalmic artery.

ICA was subsequently removed using a high-speed drill and Kerrison rongeur, allowing extension of the dissection laterally toward the CS and inferiorly toward the clivus. This technique enabled wide endoscopic exposure of the region extending to the foramen lacerum and proximal carotid ring.

For clinical correlation, the anatomical boundaries of the MC were intraoperatively identified in 20 patients undergoing endoscopic transsphenoidal surgery for pituitary adenomas with lateral and posterior CS extension. In these cases, tumor growth was initially observed within the superior compartment via the MC, followed by secondary extension into the lateral and posterior compartments. These clinical observations provided a practical framework for conceptualizing the 3D architecture and surgical relevance of the MC. The primary surgical objective in all cases was to achieve gross total tumor resection while preserving the integrity of adjacent cranial nerves (CNs) and vascular structures.

RESULTS

In all cadaveric specimens, the C4 segment of the ICA was found to terminate at the proximal dural ring, beginning at the superior margin of the petrolingual ligament encircling the artery. This segment was consistently surrounded by areolar tissue, adipose tissue, the cavernous venous plexus, and postganglionic sympathetic nerve fibers. Anatomically, the cavernous ICA was composed of a vertical segment, posterior bend (medial loop), horizontal segment, and anterior bend (anterior loop). These characteristic anatomical configurations were clearly and consistently identified in all five cadaveric specimens examined in the present study (Figure 1).

The paraclival ICA was observed to continue superiorly into the cavernous portion. The junction between the horizontal segment of the cavernous ICA and the short vertical segment extending from the posterior genu to the proximal dural ring

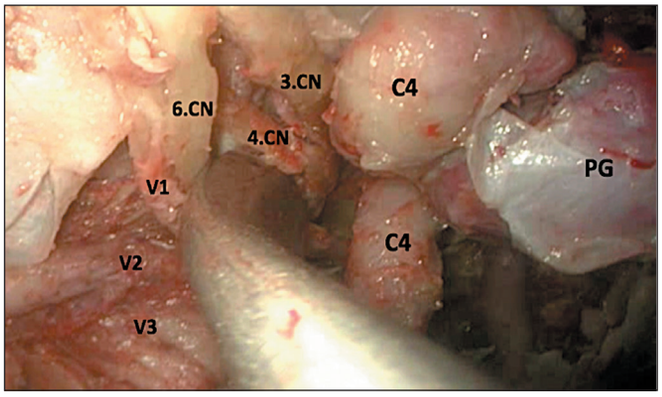

Figure 2: View when the ophthalmic branch of the trigeminal cranial nerve (CN) and the abducens CN are eliminated laterally. **C4:** cavernous segment of the internal carotid artery, **PG:** pituitary gland, **V1:** ophthalmic branch of the trigeminal CN, **V2:** maxillary branch of the trigeminal CN, **V3:** mandibular branch of the trigeminal CN.

was designated as the C4 segment. Careful stripping of the sellar dura and the dural layer overlying the ICA allowed exposure of the neurovascular structures within the CS, including the oculomotor and abducens CNs as well as the pituitary gland (Figure 2).

The neurovascular elements that were systematically examined included the oculomotor (CN III), abducens (CN VI), ophthalmic (V1), and maxillary (V2) divisions of the trigeminal nerve, and the C4 segment of the ICA. In addition, the proximal dural ring, ophthalmic artery, and optic nerve were identified. Following removal of the bone overlying the ICA, the bony lateral sellar compartment was excised to enable tracing of the CNs within the CS. The oculomotor nerve was observed coursing within the lateral wall of the CS at the level of the hor-

Table I: The measurement of the distance between the anterior genu and the pituitary gland to enter the medial corridor in the study on 5 cadavers and 10 cavernous sinuses (CS)

The measurement between the anterior genu and the pituitary gland (mm)	First cadaver	Second cadaver	Third cadaver	Fourth cadaver	Fifth cadaver	Mean±SD
Right CS	6.4	6.2	5.6	4.1	2.9	5.0±1.5
Left CS	5.9	5.3	6.8	3.2	3.4	4.9±1.6

CS: *cavernous sinus.*

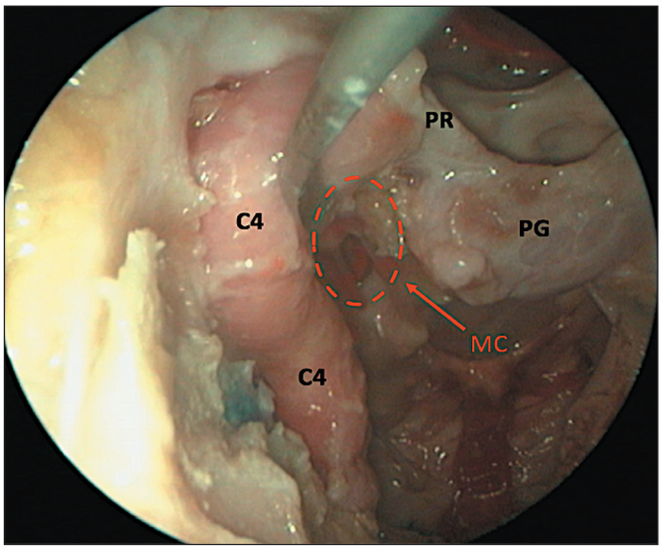

Figure 3: Examination of the medial corridor following mobilization of the cavernous segment of the internal carotid artery. **C4:** cavernous segment of the internal carotid artery, **PG:** pituitary gland, **PR:** proximal ring.

izontal ICA segment, bending around the C4 segment before entering the superior orbital fissure (SOF). The intradural segment of the oculomotor nerve was preserved unless pathological extension involved the roof or lateral wall of the CS.

The most vulnerable portion of the oculomotor nerve was consistently identified adjacent to the anterior genu of the ICA, a region that remains difficult to access through a medial-to-lateral endoscopic approach. The abducens nerve followed a trajectory corresponding to the mid-portion of the vertical C4 segment after exiting Dorello's canal, coursing near the ICA en route to the SOF. The ophthalmic division of the trigeminal nerve traveled parallel to the abducens nerve before entering the SOF. Upon lateral displacement of the abducens nerve and ophthalmic division, the trochlear nerve was identified running parallel to the oculomotor nerve. A clear visualization of the anatomical relationship between the CS and the optic nerve was obtained by opening the dura overlying the optic nerve, planum sphenoidale, and optic protuberance, and tracing it anteriorly to the optic canal (Figure 2).

The MC, as previously described by Fernandez-Miranda et al. (11), and utilized by our group to access the superior compartment of the CS, was distinctly identifiable in all specimens. The anatomical boundaries of the MC were defined superiorly by the proximal dural ring, medially by the pituitary gland, and laterally by the ICA (Figure 3).

During pituitary adenoma surgery, the oculomotor nerve, previously identified and dissected in cadaveric specimens, became visible upon entry into the MC and served as a critical lateral surgical boundary (Figure 4). To further characterize the MC, the horizontal distance between the anterior genu of the ICA and the lateral margin of the pituitary gland was measured, defining a practical entry point into the corridor (Figure 5). The mean distance was approximately 5 mm, and this may have clinical relevance for guiding safe surgical access. For comparative analysis, measurements were categorized into the following two groups: greater than 5 mm and less than 5 mm (Table I).

In the clinical series, pre- and postoperative magnetic resonance imaging of pituitary adenomas confined to the superior compartment clearly demonstrated MC involvement, supporting its role as a preferential pathway for tumor invasion, in close association with the carotid siphon (Figure 6). Intraoperatively, tumor tissue within the MC was removed using a combination of suction and curettage. As dissection progressed toward the lateral aspects of the anterior and posterior ICA segments, suction pressure was deliberately reduced to ensure safe tumor removal. Once the MC was fully exposed and tumor evacuation was completed, the oculomotor nerve was visualized laterally (Figure 7), indicating the lateral limit of the corridor. At this stage, the surgical procedure was terminated to avoid CN injury.

Across the clinical cohort of 20 patients, the patterns of CS compartment invasion, resection extent, patient age, tumor secretory status, and biochemical remission outcomes were systematically analyzed. These findings are summarized in Table II.

DISCUSSION

The CS represents one of the most anatomically intricate regions of the skull base, harboring neurovascular structures of critical functional significance. Consequently, it is a surgically formidable area. A precise understanding of the spatial relationships among the neural and vascular components within the CS is indispensable for effective surgical planning and risk mitigation. Nevertheless, any attempt to classify or compartmentalize such a complex anatomical structure inherently carries the risk of subjective interpretation and artificial boundary definition.

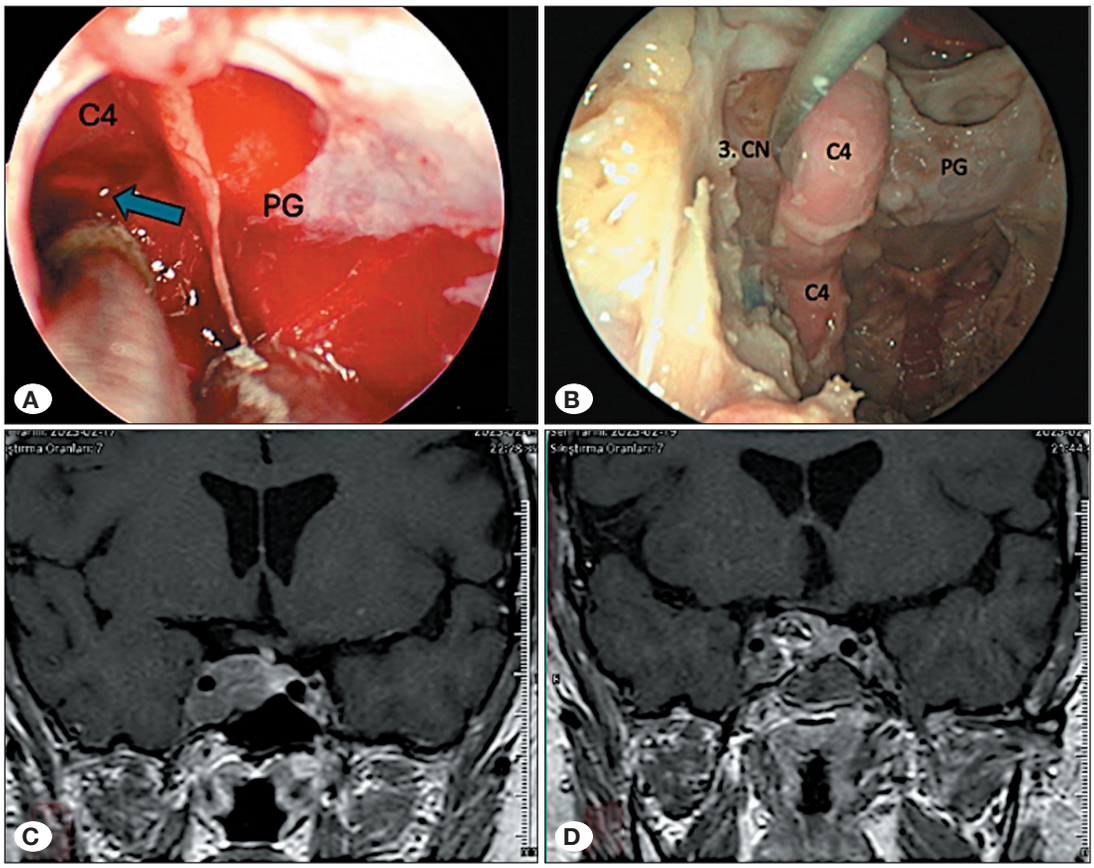

Figure 4: A) Clinical case image demonstrating the oculomotor cranial nerve (CN) indicated by an arrow, the internal carotid artery at the cavernous segment (C4), and the pituitary gland (PG). **B)** Cadaveric dissection showing the detailed anatomy of the relevant structures. **C)** Preoperative magnetic resonance imaging (MRI) revealing tumor extension into both the superior and lateral compartments of the cavernous sinus. **D)** Postoperative MRI demonstrating the absence of residual tumor within the superior and lateral compartments, corroborating intraoperative assessments and confirming the completeness of the resection.

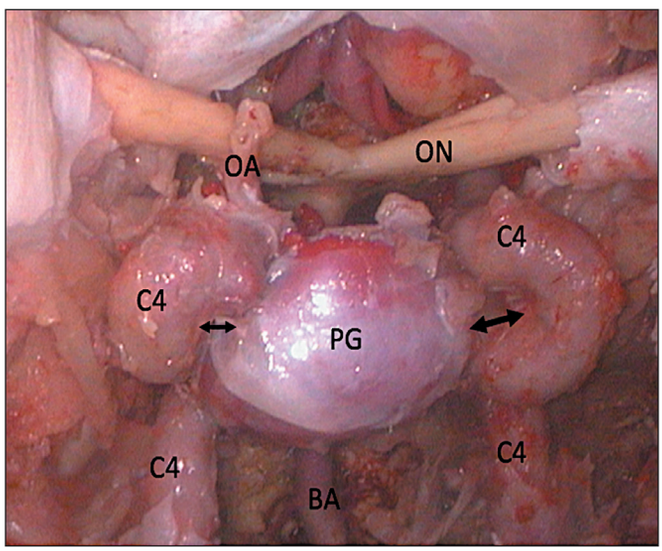

Figure 5: Horizontal measurement between the pituitary gland (PG) and the anterior genu of the cavernous segment (C4) of the internal carotid artery. **BA:** basilar artery, **OA:** ophthalmic artery, **ON:** optic nerve.

Traditionally, transcranial approaches targeting the lateral and superior walls of the CS have been favored for lesion removal. These include the subtemporal approach via the lateral wall, the pterional approach through the superior wall, the transpetrosal–transtentorial approach via the posterior wall, and the contralateral pterional–transsylvian approach through the medial wall (1). However, the effectiveness of transcranial approaches is frequently compromised by the need for brain retraction and the dense concentration of CNs, particularly the oculomotor, trochlear, and abducens nerves, traversing the lateral wall of the CS. Thus, modified endoscopic endonasal approaches through the inferior and medial walls have increasingly been recognized as safer and more anatomically favorable alternatives for CS access.

In the present study, we clearly demonstrated the consistent presence and definable anatomical boundaries of the MC using an EETA. Our findings are consistent with those of Kitano et al. (16), who described a vertical dural incision extending from the posterior to the anterior aspect of the cavernous ICA through the MC, allowing tumor resection up to the superior wall of the CS. In contrast, our technique employed a transverse dural incision with window-shaped dural excision, facil-

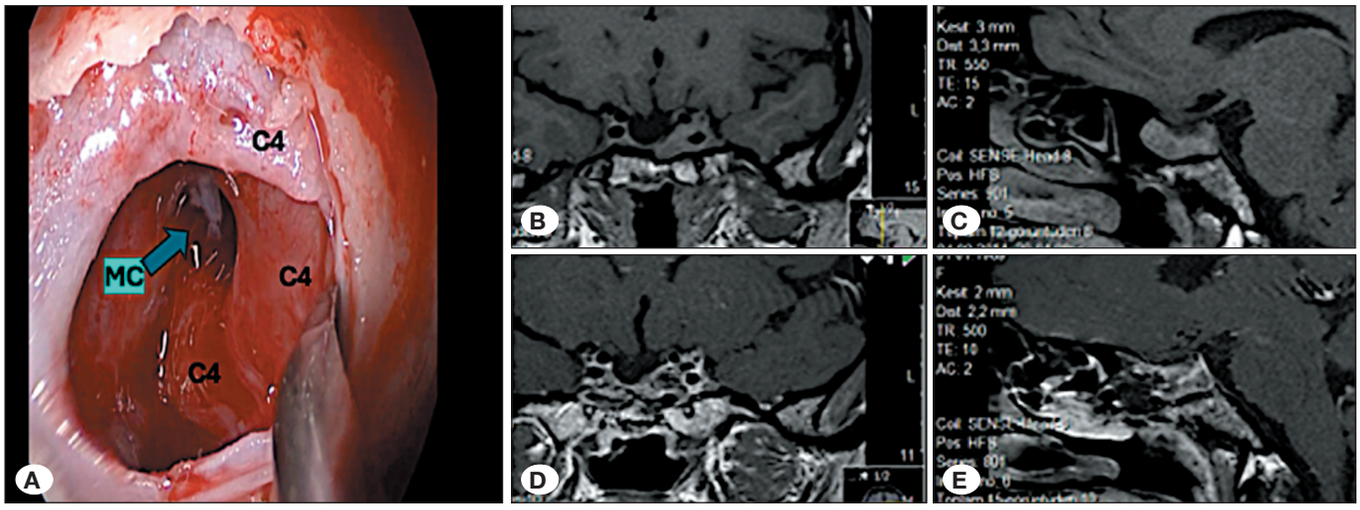

Figure 6: Perioperative **(A)** demonstration of the medial corridor (MC) in one of the cases from our clinical series, along with pre- **(B,C)** and postoperative **(D,E)** magnetic resonance imaging of the same case. **C4:** cavernous segment of the internal carotid artery.

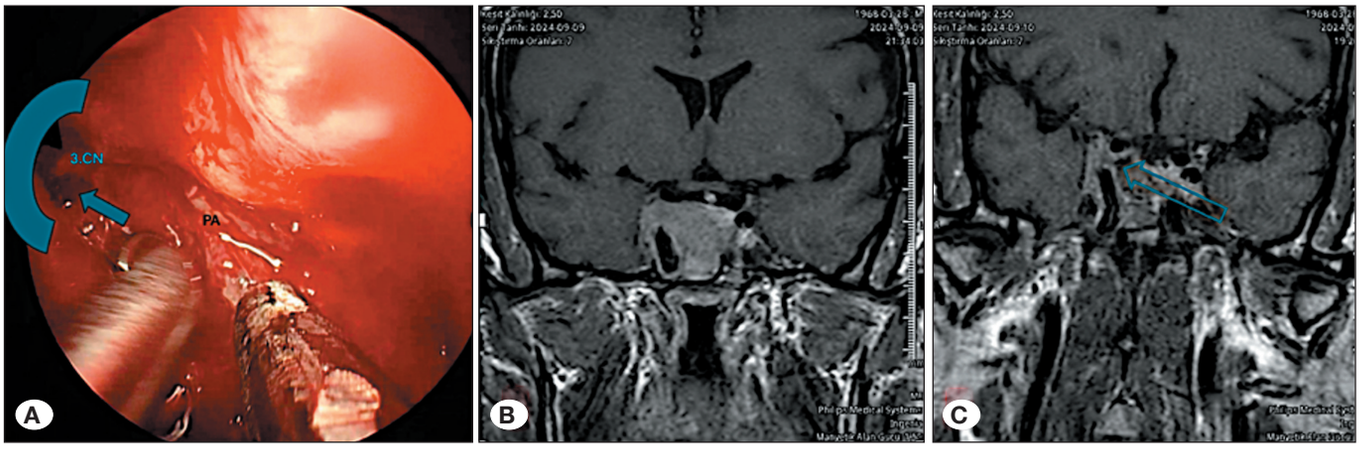

Figure 7: A) The thick C-shaped structure represents the internal carotid artery siphon (C4). The arrow points to the medial corridor (MC), whose lateral boundary is the third cranial nerve (3rd CN). **B)** Preoperative magnetic resonance imaging (MRI) demonstrating tumor extension into the medial corridor. **C)** Postoperative MRI confirming gross total resection of the tumor. **PA:** pituitary adenoma.

itating direct visualization of the spatial relationship between normal pituitary tissue and the posterior genu, horizontal segment, and anterior genu of the ICA. When advancing through the intersegmental space between these ICA components via the MC, the oculomotor nerve was consistently encountered, defining the lateral boundary of the corridor. Accordingly, we propose that intraoperative visualization of the oculomotor nerve during tumor excision within the MC reliably indicates that the lateral extent of safe resection has been reached.

In typical clinical settings, the oculomotor nerve is often visualized indirectly as a reflexive structure during CS surgery. However, in the clinical cases included in our study, invasive tumors occupied the CS and infiltrated its lateral wall, enabling direct and unambiguous visualization of the third CN. This finding underscores the practical surgical relevance of the MC in cases of advanced CS involvement.

Theodosopoulos et al. emphasized that the distance between the ICA and the pituitary gland plays a pivotal role in facilitating access to the lateral CS, and they introduced the concept of a “wide-area” MC (19). Our findings corroborate this observation, particularly in cases where the pituitary gland remains uninvolved and tumor extension is confined to the CS. In the present cadaveric series, a threshold distance of approximately 5 mm between the anterior genu of the ICA and the lateral margin of the pituitary gland was found to be a clinically meaningful parameter. When this distance was ≥5 mm, entry into the MC was consistently more feasible, and controlled ICA manipulation could be performed with greater safety.

It is well recognized that many nonfunctioning pituitary adenomas extending toward the CS are neither biologically aggressive nor truly invasive (18), a phenomenon often attributed to tumor growth through structurally weak regions of the CS

Table II: Distribution of cavernous sinus compartment invasion, extent of resection, age, hormonal activity (secretory vs. non-secretory), and remission status of 20 patients included in the series

Gender	Age (years)	Hormone secretion	Cavernous Sinus Invasion – Compartment	Complication	Resection	Remission
M	28	GH	Superior-Posterior	None	NT	No
M	34	GH	Superior	None	GT	Yes
F	23	NS	Posterior	None	GT	–
F	33	GH	Superior-Posterior	None	ST	No
M	37	PRL	Superior	None	GT	Yes
F	50	GH	Superior	None	GT	Yes
F	29	NS	Superior-Posterior	CSF Leak	GT	–
M	27	GH	Superior	None	GT	Yes
M	37	GH	Superior-Posterior	None	NT	No
M	27	GH	Superior	None	GT	Yes
M	57	GH PRL	Superior, Anteroinferior, Posterior	Epistaxis	ST	No
F	40	GH	Superior	None	GT	Yes
F	28	GH	Superior	None	GT	Yes
M	40	NS	Superior-Posterior	None	NT	–
M	46	NS	Superior-Posterior	None	GT	–
M	37	GH	Superior	None	GT	Yes
M	33	NS	Superior-Posterior	None	GT	–
F	44	NS	Superior	None	GT	–
F	36	GH	Superior	None	NT	No
M	29	GH	Superior	None	GT	Yes

GH: *growth hormone,* ***PRL:*** *prolactin,* ***NS:*** *non-secreting,* ***CSF:*** *cerebrospinal fluid,* ***GT:*** *gross total,* ***NT:*** *near total,* ***ST:*** *subtotal,* ***M:*** *male,* ***F:*** *female.*

wall. Clinical series have demonstrated that when pituitary adenomas invade the CS, progression most commonly occurs via the MC (5,13). At present, no neuroimaging modality allows definitive visualization of the medial wall of the CS. Anatomical studies have variably described this structure as single-layered, double-layered, or thin and loosely organized with focal histological defects (7,9,10). Consequently, while some authors have emphasized tumor histology as the primary determinant of CS invasion, others have highlighted the inherent structural vulnerability of the medial wall as the key facilitating factor (9).

Pituitary adenomas may originate within either the medial or lateral corridors of the cavernous ICA. Lesions extending laterally within the CS frequently invade the anteroinferior ICA region or the MC. Songtao et al. (17) demonstrated that the lamina propria lines the inner surface of the pituitary gland, while the pituitary capsule envelops its outer surface, with the inferolateral capsule being relatively thick and the medial wall being structurally weaker. Following invasion of the lamina propria and pituitary capsule, adenomas may exploit these weak points of the medial wall and extend along the characteristic C-shaped course of the ICA, thereby creating a surgically exploitable endoscopic corridor medial to the cavernous ICA (2). The present series also illustrates a notable anatomical variation in which the horizontal ICA segment coursed unusually close to the midline (Figure 8), further emphasizing the importance of individualized anatomical assessment.

Multiple surgical corridors between neurovascular structures have been described to facilitate endoscopic access to the CS. Corridors lateral to the ICA are generally more directly accessed via ipsilateral expanded endonasal or far-lateral transethmoidal or transsphenoidal approaches. In contrast, the MC of the ICA was more effectively explored through a contralateral endoscopic route, consistent with prior anatomical and clinical studies. In a representative case, advancement through the MC enabled access to the lateral compartment via meticulous dissection along the lateral aspect of the ICA (Figure 9).

From a surgical standpoint, the MC represents the only endoscopic route capable of addressing lesions extending from the sella into the lateral CS while displacing the CNs and ICA laterally, thereby providing access to the lateral sellar compartment (16).

Despite these findings, several limitations inherent to cadaveric studies must be acknowledged. Differences in tumor consistency, prior treatment effects, displacement of neurovascular structures, and anatomical variability of the ICA within the CS may limit direct clinical extrapolation. Most notably, the absence of tumor tissue within the CS in cadaveric speci-

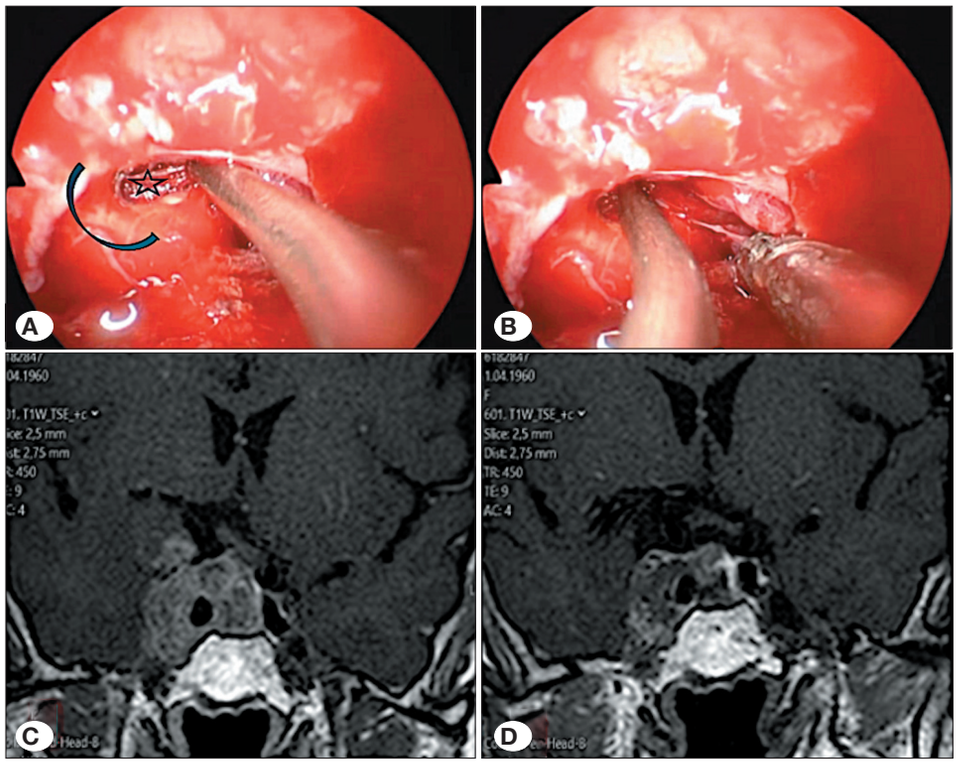

Figure 8: A) This case presents a variation in the anatomy of the internal carotid artery. The tumor is excised by directly accessing the superior and lateral compartments through the medial corridor (MC). Atherosclerotic changes within the horizontal segment extending toward the midline are clearly observed. The medial corridor is delineated by dense fibrotic bands, marked with a star. **B)** The tumor tissue is accessed via the MC using an aspirator, and surgical excision is performed. **C,D)** Pre- and postoperative magnetic resonance imaging demonstrating the tumor status before and after resection.

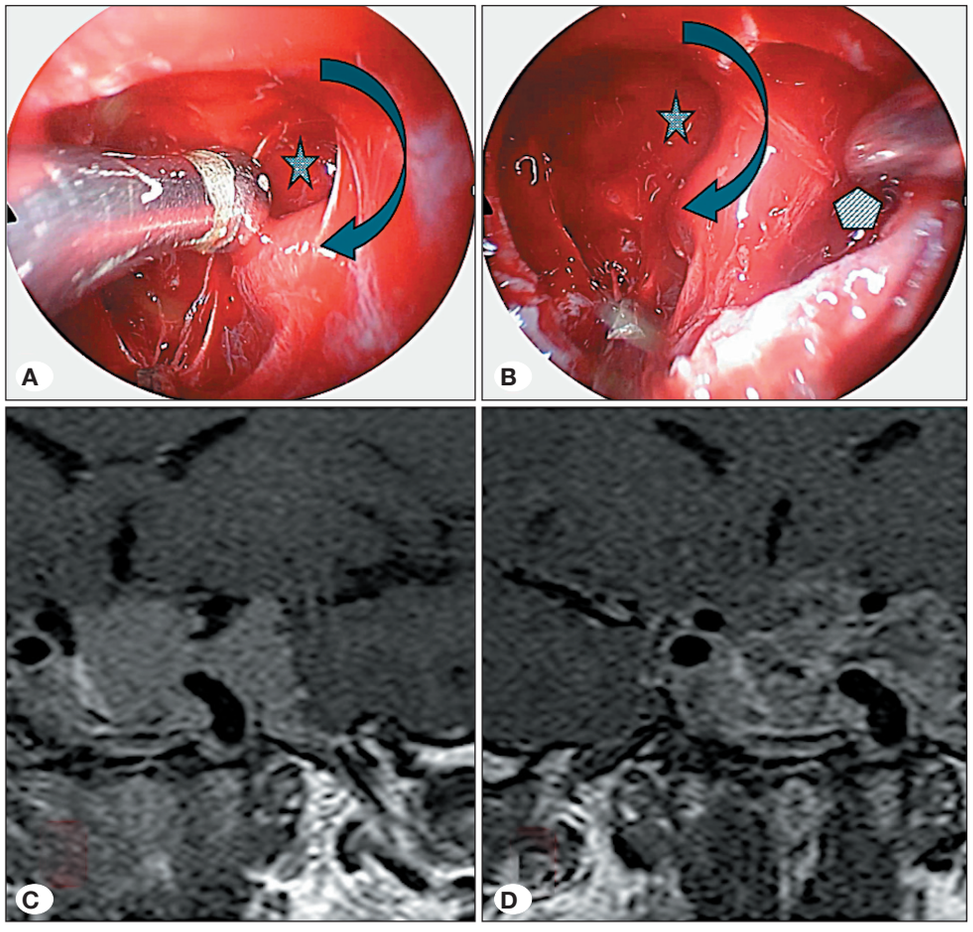

Figure 9: Tumor extension and surgical approaches. In the present case, the tumor extends into the superior and lateral compartments. **A)** The anterior and horizontal segments of the cavernous segment of the internal carotid artery are exposed. Entry is achieved via the medial corridor (marked with a star), allowing access to the tumor located in the superior compartment using an aspirator. **B)** Surgical dissection proceeds laterally to the cavernous segment of the internal carotid artery, and the tumor tissue within the lateral compartment (marked with a pentagon) is accessed and excised. **C,D)** Pre- and postoperative magnetic resonance imaging findings.

mens precludes the assessment of tumor-induced distortion, compression, and fibrotic adhesions that affect critical neurovascular elements. Consequently, the applicability of anatomical observations may vary depending on the extent of tumor invasion and the degree of neurovascular displacement encountered in clinical practice.

CONCLUSION

We have provided a precise anatomical definition and reproducible delineation of the MC using the EETA. The anatomical and clinical findings of this study support the concept that the MC represents a fundamental and preferential pathway for the extension of pituitary adenomas and other intrasellar lesions into the superior, lateral, and posterior compartments of the CS. As such, the MC should be regarded not merely as a surgical access route but as a critical anatomical interface that governs both tumor invasion dynamics and the limits of safe endoscopic resection.

We further demonstrated that the approximately 5-mm interval between the anterior genu of the ICA and the lateral margin of the pituitary gland constitutes a pivotal anatomical determinant at the entry point of the MC. This spatial parameter appears to directly influence surgical accessibility to the MC and the adjacent CS compartments, thereby defining a practical threshold for safe and controlled endoscopic advancement. By integrating high-resolution anatomical measurements with intraoperative and radiological clinical correlations, the findings of our study underscore that a nuanced, quantitative understanding of MC anatomy is indispensable for refining surgical decision-making, maximizing the extent of safe tumor removal, and minimizing the risk of neurovascular morbidity. Collectively, the findings of this study position the MC as a central anatomical and surgical concept in contemporary endoscopic CS surgery.

ACKNOWLEDGEMENTS

The authors express their gratitude to the Bahcesehir University Rhoton Anatomy Laboratory for supplying the cadaveric specimens used in this study.

We also wish to acknowledge the medical staff who contributed to the surgical procedures and data collection for the clinical cases.

Declarations

Funding: This research did not receive any specific grant from funding agencies in the public, commercial, or not-for-profit sectors.

Availability of data and materials: The datasets generated and/or analyzed during the current study are available from the corresponding author by reasonable request.

Disclosure: The authors declare no competing interests.

AUTHORSHIP CONTRIBUTION

Study conception and design: BC, SC
Data collection: AG, AU, EY, AE, MC
Analysis and interpretation of results: AG, BC, IA
Draft manuscript preparation: AG, AU
Critical revision of the article: SC
Other (study supervision, fundings, materials, etc...): SC, AG
All authors (AG, AU, EY, AE, MC, BC, IA, SC) reviewed the results and approved the final version of the manuscript.

REFERENCES

1. Cappabianca P, Alfieri A, de Divitiis E: Endoscopic endonasal transsphenoidal approach to the sella: Towards functional endoscopic pituitary surgery (FEPS). Minim Invasive Neurosurg 41:66-73, 1998. https://doi.org/10.1055/s-2008-1052019
2. Cavallo LM, Cappabianca P, Galzio R, Laconetta G, de Divitiis E, Tschabitscher M: Endoscopic Transnasal Approach To The Cavernous Sinus Versus Transcranial Route: Anatomic Study. Neurosurgery 56:279-389, 2005. https://doi.org/10.1227/01.NEU.0000156548.30011.D4
3. Ceylan S, Anik I, Cabuk B, Caklili M, Anik Y: Extension Pathways of Pituitary Adenomas with Cavernous Sinus Involvement and Its Surgical Approaches. World Neurosurgery 127:986-995, 2019. https://doi.org/10.1016/j.wneu.2019.04.013
4. Ceylan S, Anik I, Koc K, Cabuk B: Extended endoscopic transsphenoidal approach infrachiasmatic corridor. Neurosurg Rev 38:137-147, 2015. https://doi.org/10.1007/s10143-014-0576-0
5. Ceylan S, Koc K, Anık I: Endoscopic endonasal transsphenoidal approach for pituitary adenomas invading the cavernous sinüs. J Neurosurg 112:99-107, 2010. https://doi.org/10.3171/2009.4.JNS09182
6. Ceylan S, Sen HE, Ozsoy B, Ceylan EC, Ergen A, Selek A, Anik Y, Balci S, Cabuk B, Anik I: Endoscopic approach for giant pituitary adenoma: clinical outcomes of 205 patients and comparison of two proposed classification systems for preoperative prediction of the extent of resection. J Neurosurg 136:786-800, 2022. https://doi.org/10.3171/2021.3.JNS204116
7. Ciric I. On the origin and nature of the pituitary gland capsule. J Neurosurg 46:596-600, 1977. https://doi.org/10.3171/jns.1977.46.5.0596
8. de Divitiis E, Cappabianca P, Cavallo LM: Endoscopic transsphenoidal approach: Adaptability of the procedure to different sellar lesions. Neurosurgery 51:699-707, 2002. https://doi.org/10.1097/00006123-200209000-00016
9. Dolenc VV: Anatomy and surgery of the cavernous sinus. Springer, Berlin, 1989. https://doi.org/10.1007/978-3-7091-6942-1
10. Dolenc VV: Relation of the cavernous sinus to the sella. In: Dolenc VV (eds), Anatomy and surgery of the cavernous sinus. Vienna: Springer-Verlag, 1989:118-130, 1989. https://doi.org/10.1007/978-3-7091-6942-1

11. Fernandez-Miranda JC, Gardner P, Snyderman C: Endoscopic endonasal trans cavernous posterior clinoidectomy with interdural pituitary transposition. J Neurol Surg B Skull Base 75: A022, 2014. https://doi.org/10.3171/2014.3.JNS131865
12. Fermandez-Miranda JC, Zwagerman NT, Abhinav K, Lieber S, Wang EW, Snyderman CH, Gardner PA: Cavernous sinus compartments from the endoscopic endonasal approach: anatomical considerations and surgical relevance to adenoma surgery. J Neurosurgery 129:430-441, 2018. https://doi.org/10.3171/2017.2.JNS162214
13. Frank G, Pasquini E: Endoscopic endonasal approaches to the cavernous sinus: Surgical approaches. Neurosurgery 50:675, 2002. https://doi.org/10.1097/00006123-200203000-00059
14. Harris FS, Rhoton AL Jr. Anatomy of the cavernous sinus: A microsurgical study. J Neurosurg 45:169-180, 1976. https://doi.org/10.3171/jns.1976.45.2.0169
15. Jho HD, Ha HG: Endoscopic endonasal skull base surgery: Part 2-The cavernous sinus. Minim Invasive Neurosurg 47:9-15, 2004. https://doi.org/10.1055/s-2004-818346
16. Kitano M, Taneda M, Shımono T, Nakao Y: Extended transsphenoidal approach for surgical management of pituitary adenomas invading the cavernous sinus. J Neurosurg 108:26-36, 2008. https://doi.org/10.3171/JNS/2008/108/01/0026
17. Songtao Q, Yuntao L, Jun P, Chuanping H, Xiaofeng S: Membranous layers of the pituitary gland: a histological anatomic study and related clinical issues. Neurosurgery 64:1-10, 2009. https://doi.org/10.1227/01.NEU.0000327688.76833.F7
18. Taniguchi M, Hosoda K, Akutsu N, Takahashi Y, Kohmura E: Endoscopic endonasal transsellar approach for laterally extended pituitary adenomas: Volumetric analysis of cavernous sinus invasion. Pituitary 18:518-524, 2015. https://doi.org/10.1007/s11102-014-0604-7
19. Theodosopoulos PV, Cebula H, Kurbanov A, Cabero AB, Osorio JA, Zimmer LA, Froelich SC: The medial extra-sellar corridor to the cavernous sinus: Anatomic description and clinical correlation. World Neurosurg 96:417-422, 2016. https://doi.org/10.1016/j.wneu.2016.09.046